Distribution Agreement

In presenting this thesis as a partial fulfillment of the requirements for a degree from Emory University, I hereby grant to Emory University and its agents the non-exclusive license to archive, make accessible, and display my thesis in whole or in part in all forms of media, now or hereafter now, including display on the World Wide Web. I understand that I may select some access restrictions as part of the online submission of this thesis. I retain all ownership rights to the copyright of the thesis. I also retain the right to use in future works (such as articles or books) all or part of this thesis.

Aliyah Auerbach April 14, 2020

Neural Plasticity in the Lateral Geniculate Nucleus Following Lesion to the Primary Visual Cortex in Macaque Monkeys

by

Aliyah Auerbach

Hillary Rodman, PhD

Adviser

Neuroscience and Behavioral Biology

Hillary Rodman

Adviser

Kristen Frenzel

Committee Member

Bradley Howard

Committee Member

2020

Neural Plasticity in the Lateral Geniculate Nucleus Following Lesion to the Primary Visual Cortex in Macaque Monkeys

By

Aliyah Auerbach

Hillary Rodman

Adviser

An abstract of
a thesis submitted to the Faculty of Emory College of Arts and Sciences
of Emory University in partial fulfillment
of the requirements of the degree of
Bachelor of Science with Honors

Neuroscience and Behavioral Biology

2020

Abstract

Neural Plasticity in the Lateral Geniculate Nucleus Following Lesion to the Primary Visual Cortex in Macaque Monkeys

By Aliyah Auerbach

Following lesion to primary visual cortex (V1) in macaque monkeys, retrograde degeneration occurs in neurons that project to V1 in the lateral geniculate nucleus (LGN). Lesion of V1 results in blindness to the visual field. Despite this "blindness", certain individuals retain residual visual capacity allowing them to implicit decisions about stimuli without awareness of their presence, a condition called blindsight. This remaining visual function is thought to be mediated by the LGN, in which interlaminar cells are implicated. We sought to determine what mediates the survival of these primarily calbindin-rich interlaminar LGN neurons following V1 lesion. Six macaque monkeys were used, four lesioned at infancy and two at adulthood. We hypothesized that surviving cells in the LGN survive because of their proximity to blood vessels. Our prediction was that the distance of a surviving cell from the nearest blood vessel in the degenerated LGN to be less than expected by chance and to be less than that of randomly selected cells in the corresponding intact LGN section. Our second hypothesis was that cells that fall within a zone of high retinal innervation are more likely to survive degeneration and we predicted that surviving cells would be preferentially located in an area of high retinal input compared with randomly selected cells in the intact LGN. Our results showed that surviving cells were not significantly closer to blood vessels than by chance or in the correlated intact LGN, and only one of the five subjects showed significant preferential clustering in areas of high retinal innervation post-lesion. Therefore, the results of our experiments did not support either hypothesis. However, we did find that adult-lesion surviving cells were significantly closer to blood vessels than infant-lesion surviving cells post-lesion and adult-lesion animals contained a

significantly higher proportion of calbindin-negative surviving cells than infant-lesion animals. As such, future directions could involve looking further into distinguishing characteristics of these calbindin-negative cells that survive, the effects of age and other individual differences that may account for these results, and possible dendritic branching of surviving cells post-lesion.

Neural Plasticity in the Lateral Geniculate Nucleus Following Lesion to the Primary Visual Cortex in Macaque Monkeys

By

Aliyah Auerbach

Hillary Rodman

Adviser

A thesis submitted to the Faculty of Emory College of Arts and Sciences
of Emory University in partial fulfillment
of the requirements of the degree of
Bachelor of Science with Honors

Neuroscience and Behavioral Biology

2020

Acknowledgements

I would like to thank Dr. Hillary Rodman for her constant support and counsel throughout this process and my time in her laboratory. I would like to thank Dr. Hillary Rodman, Dr. Kristen Frenzel, and Professor Bradley Howard for being members of my committee and taking part in my thesis experience. I would like to thank my colleague Anna Ree for her assistance in data collection. Sections for these analyses were drawn from material prepared by Kristy Sorenson and Hye Mee Na. This work was supported by NSF IBN-9723178 and NIH RR00165.

Table of Contents

Introduction 1
Blindsight and Behavior 1
Relevant Neuroanatomy of the Visual System 3
Hypotheses and Predictions 6
Materials and Methods 8
Results 12
Discussion 14
Distance from Blood Vessel Hypothesis 14
Retinal Innervation Hypothesis 17
Implications, Future Directions, and Conclusion 19
Tables and Figures 23
Table 1: Table of identifying information for all six subjects 23
Figure 1: Diagram of the primary and secondary visual pathways 24
Figure 2: Representative section of the unlesioned LGN of subject RMS-3 25
Figure 3: Comparison of overall average distance from blood vessels in both spared cells and corresponding random points for all infant-lesion cases 26
Figure 4: Comparison of overall average distance from blood vessels in both spared cells and corresponding random points for all adult-lesion cases 27
Figure 5: Comparison of distance from surviving cell to blood vessel in degenerated LGN of both infant- and adult-lesion cases 28
Figure 6: Comparison of surviving calbindin-positive cells in the degenerated LGN to randomly selected calbindin-positive cells in the intact LGN 29
Figure 7: Classification of surviving cells in adult-lesion animals: calbindin-positive or negative 30
Figure 8: Classification of surviving cells in adult-lesion animals: calbindin-positive or negative 31
Figure 9: Average difference in percentage of surviving cells in area of high retinal innervation across all sections 32
Figure 10: Comparison of cell location distribution in the DEZ of intact LGN and corresponding surviving calbindin-positive cells in degenerated LGN for all infant-lesion subjects 33
References 34

Introduction

Blindsight and Behavior

In both humans and primates, visual capacity plays an important role in survival. Since the age of hunter-gatherers, higher quality vision has corresponded to advantageous behaviors adapted to both predator and prey – allowing predators to be able to easily spot a meal and gifting prey a more evolved visual warning system. These abilities can be compromised by traumatic brain injury, resulting in widespread deleterious effects on the evolutionary fitness of that individual. Unsurprisingly, there are a multitude of neural structures responsible for various aspects of the visual experience. Our study focuses on the neural plasticity of one of these structures, the lateral geniculate nucleus, following lesion to the primary visual cortex in macaque monkeys.

Following lesion to the primary visual cortex, retrograde degeneration occurs throughout the visual system (described in the next section). Despite the damage caused post-V1 lesion, there can be significant mediation of visual capacity in areas of the visual field in which blindness is present. This limited visual capacity allows an affected person to make implicit decisions about the nature of stimuli without being consciously aware of their presence, a condition known as blindsight. Blindsight examines a dichotomy between vision and awareness in which animals can "see" an object they are perceptually unaware of. Most blindsight patients are able to detect and discriminate stimuli based upon attributes like movement (Riddoch, 1917), physical orientation (Chariker et al., 2016), and shape discrimination (Dineen & Keating, 1981).

Blindsight patients are often tested in scenarios in which they must identify the shape, direction of movement, and location of a stimulus through a forced-choice procedure. This procedure forces the subject to indicate which one of a set number of spatial or temporal

intervals contain[s] the stimulus and does not give them an option to indicate that they cannot see the stimulus. In contrast, yes-no testing asks the subject whether they saw a stimulus and provides the option to say no stimulus was observed. This circles back to the concept of vision without awareness, as the average performance of a blindsight patient is ~50% correct with the yes-no paradigm but ~90% correct with the forced-choice paradigm (Azzopardi and Cowey, 1998). This performance can be interpreted as equivalent to chance in the yes-no paradigm, whereas 90% far exceeds the chance one would expect by chance in the forced-choice paradigm. The dichotomy in accuracy is immensely interesting when one considers that the subject continuously "denies any visual awareness of the target" (Azzopardi and Cowey, 1998), despite being able to observe movement of the stimulus in a forced-choice environment.

A complication arises when testing monkeys for blindsight in that, unlike humans, they cannot verbally confirm or deny seeing a stimulus. In an experiment conducted by Gross et. al., six *Macaca fascicularis* monkeys underwent a forced-choice paradigm in which visually guided behaviors -- specifically saccadic eye movements – were being observed for blindsight-like behaviors. Each subject received a large unilateral striate cortex lesion either in infancy (5-6 weeks of age) or in adulthood. Following lesion, they were tested on their ability to successfully make saccades to visual targets. In order to receive an award, the animal had to both detect the onset of the stimulus and make a saccade to it. The results from this experiment show that animals in both groups (adult-lesion and infant-lesion) perform with almost perfect accuracy in the visual field ipsilateral to the striate cortex lesion. While the infant-lesioned animals were still relatively efficient in detecting and localizing stimuli in their impacted visual field, the adult-lesioned animals exhibited blindness in that visual hemifield after many repetitions. However, experimenters noted that these adult-lesion animals were still aware of target location and, in a

follow-up experiment, were shown capable of making saccades to the target point if the fixation point was turned off when the target appeared. By doing so, the monkey is "forced" to find a new fixation point and lands with significant accuracy on the target points in the contralateral visual field.

Relevant Neuroanatomy of the Visual System

The intact primary visual pathway (as shown in Figure 1) in primates entails visual information entering the brain via the retina and travelling along the optic nerve to the primary visual cortex. The optic nerve feeds into the optic chiasm where visual input is divided into input from the left and right visual fields, with information from the left visual field localized in the right hemisphere and vice versa. The organized visual information then travels via the optic tract to the lateral geniculate nucleus (LGN), a six-layered structure present in both hemispheres, its primary purpose being the transfer of retinal input to striate cortex (V1). The superior colliculus and pulvinar are other targets also innervated by the optic tract and are involved in secondary visual pathways.

Lesion to the primary visual cortex (V1) in primates results in retrograde degeneration of neurons that project to V1. This occurs in the lateral geniculate nucleus (LGN) on the same side (ipsilateral) as this lesion. The resultant degeneration involves projection neurons in the magnocellular (M), parvocellular (P), and koniocellular (K) layers of the LGN (as described further below). Previous studies have shown the degeneration of the ipsilateral LGN to occur within a 6-month period and to comport with a 50% decrease in size relative to the unaffected LGN regardless of age of onset (Atapour et al., 2017).

Additional studies suggest a difference in performance ability based on age of lesioning in which infant-lesion animals consistently perform better on saccadic target localization tests

than their adult-lesion counterparts (Gross et al., 2004). Our study utilizes tissue from both adult- and infant-lesion macaque monkeys and thus the difference in recovery efficiency between infants and adults comes into play following traumatic brain injury. In the Gross et al. study aforementioned, the infant-lesioned animals consistently make more accurate and timely saccades to a target point than their adult-lesioned counterparts. Additionally, this degeneration seems to occur at a faster pace and cause more damage in infants than adults, which comports with the increased vulnerability of immature neurons to stress factors that cause neuronal death (Pfisterer and Khodosevich, 2017).

Macaque monkeys are frequently used as an animal model in V1 lesion projects due to the similarity of the retinotopic and laminar organization of their lateral geniculate nucleus. Both the primate and human LGN consist of six cellular layers organized with regards to source of input and type of cell primarily present. As shown in Figure 2, these layers are identified from one to six, with the first layer starting at the most ventral point of the LGN. The first two layers (colored orange in Figure 2) are primarily composed of magnocellular cells - large-bodied neurons with thick axons and large receptive fields. These magnocellular layers are implicated in motion detection and depth perception. The magno- cells populating these layers comprise ~10% of the LGN's neuronal population (Kaas et al., 1978). Layers three through six (colored blue in Figure 2) consist of parvocellular cells, smaller-bodied cells with thinner axons and small receptive fields. These cells indicate modulation in the color and form of objects; in primates, parvocellular cells comprise 80% of all LGN neurons and constitute the largest neuronal population in the LGN (Carsten et al., 2016).

The third ganglion cell type, the koniocellular/interlaminar cell, is typically intermediate in size. These cells are typically clustered in the zones between layers named the interlaminar

zones (indicated in Figure 2) and are distinguishable from magno- and parvo- ganglion cells through the presence of the calcium-binding protein, calbindin-D28k. Despite contributing 10% to the LGN's neuronal population and thus being approximately the same size as the magnocellular population, this cell type has not been studied as extensively. Notwithstanding, these cells seem to have a multitude of functions: in marmoset and owl monkeys, koniocellular layers show high sensitivity to temporal frequency flicker (Percival et al., 2014), and, in intact marmoset monkeys, these cells are thought to display high contrast sensitivity and rapid, transient responses to light onset and offset (Eiber et al., 2018). They have also been established in coding the contrast between blue and yellow-specific color perception (Percival et al., 2014).

Following lesion to V1 in macaque monkeys, degeneration-surviving cells of the LGN tend to be clustered in these interlaminar layers and test positive for calbindin, a neuroprotective calcium-binding protein that serves as a marker for koniocellular cells (Rodman et al., 2001). Moreover, 95% of the surviving neurons found in the degenerated LGN of an infant macaque monkey contained the calbindin marker for the koniocellular pathway. This suggests that remaining visual capacity may be partially mediated by primarily calbindin-positive koniocellular cells. As such, the calbindin-positive surviving cells were the focus of this experiment.

The previously dominant hypothesis was that remaining visual capacity originated from a secondary pathway that entirely bypassed the LGN, instead following a path from the retina to the superior colliculus to the pulvinar and finally to extrastriate cortex (Yu et al., 2018). This explanation of blindsight completely excludes the LGN, suggesting that there are no surviving projections originating in the LGN post-V1 lesion that allow for any mediation of visual capacity. However, deactivating the LGN when V1 has been lesioned abolishes residual vision

(Schmid et al., 2011). This leads to an alternative explanation in which the population of surviving calbindin-rich interlaminar cells in the LGN that survive degeneration and project directly to extrastriate cortex are responsible for the retention of some degree of visual function (Rodman et al, in prep). Marmoset monkeys seem to display this phenomenon, as their koniocellular LGN layers have been implicated in projecting to the middle temporal (MT) lobe and bypassing V1 altogether following damage to striate cortex (Hendrickson et al., 2015).

Hypotheses and Predictions

Our project sought to understand how these primarily calbindin-rich neurons in the LGN are able to survive degeneration. We attempted to determine which neural processes in the primary visual pathway mediate this residual visual capacity in adult- and infant-lesion macaque monkeys following lesion to the primary visual cortex. This project focused on whether either of the following two factors affect the likelihood of a calbindin-rich interlaminar LGN neuron surviving V1 lesion-prompted degeneration.

The first factor is the distance of the neuron body and its dendrite(s) from the nearest blood vessel. Blood vessels supply neurons with essential oxygen and glucose from the blood stream, and normal neuronal functioning relies on the sustainability and accessibility of vasculature (Andreone, Lacoste, & Gu, 2015). In cases of impaired central nervous system angiogenesis, there is significantly reduced tissue growth and viability presumably due to the lack of oxygen and nutrients supplied by blood vessels (Eichmann and Thomas, 2013). As such, we hypothesized that the distance from a surviving cell to the nearest blood vessel would be significantly less than the distance to the nearest blood vessel from a random point in the tissue. This hypothesis can be broken up into two subdivisions.

Are the surviving, calbindin-positive cells in the degenerated LGN (dLGN) taking better advantage of blood vessels than the calbindin-positive cells of the intact LGN? The expected outcome was that surviving cells in the degenerated LGN would be those that are taking fuller advantage of nearby blood vessels than those in the intact LGN. Additionally, are the surviving calbindin-positive cells in the degenerated LGN closer to blood vessels than would be expected by chance? We hypothesized that surviving calbindin-positive cells in the degenerated LGN would be closer to blood vessels than would be expected by chance.

The second factor we hypothesized to be involved in the survival of LGN neurons post-lesion was location of the surviving calbindin-positive neuron in relation to areas of high retinal input. Since each LGN receives input from both eyes, there is stratification of that input dependent upon which eye it originates from. In the left LGN, the right (contralateral) eye will feed retinal input to layers 1, 4, and 6. In the same left LGN, the left (ipsilateral) eye will provide retinal input to layers 2, 3, and 5. In an intact animal, input to the interlaminar layers is negligible; however, there is significant reorganization of retinal input to the degenerated LGN following V1 lesion. Previous studies have shown that, in macaque monkeys following V1 lesion, there is a significant increase in patchy retinal innervation to the interlaminar zone between layers 2 and 3 in the contralateral eye. This is indicative of cortical plasticity in the retinotopic representation of the LGN, which may correspond with the location of the calbindin-positive neurons that survive. We hypothesized that the proportion of innervation-privileged neurons (surviving neurons that fall within zones of high retinal input) would be significantly greater than the proportion that fall outside of these zones (indicative of preferential clustering) and greater than the proportion that falls within this zone in the corresponding intact LGN.

Materials and Methods

The project utilizes brain tissue previously obtained from six macaque monkeys who were lesioned in V1 at infancy (5-6 weeks, 4 subjects) or at adulthood (2 subjects). In these six animals, a unilateral lesion of central V1 was placed in the left hemisphere.

As V1 is compromised by lesion and no longer sends visual signals forward, an area of perceived blindness occurs in the visual field. Known as the scotoma, this impacted area of the visual field varies depending on which area of V1 is lesioned. For example, lesioning a large area of central V1 affects the center of vision, the point of highest visual acuity, while lesioning a smaller portion in the peripheral V1 would affect a larger mass of the peripheral visual field. Following V1 lesion there is emergence of a degenerated region in the affected LGN, referred to as the degenerated zone. The portion of the intact LGN that corresponds with this area is referred to as the degeneration equivalency zone (DEZ).

Coronal sections in series for each of these cases were previously prepared via immunohistochemistry for calbindin (the calcium-binding protein marker for the koniocellular pathway), and Giemsa staining. Giemsa staining was used in order to darken the immunoreactive product, resulting in a visible stain that revealed the cell layers of the LGN. Double-labelled material (labelling with both Giemsa and calbindin) was used to visualize distance between dendrites of surviving cells and the nearest blood vessels. Double-labelling serves three functions in this experiment: it identifies cells that send projections to the region of the brain where the tracer was placed, stains cells that project to V4, and provides high visibility of dendrites.

Approximately 8 sections per hemisphere were analyzed. This subset of sections in each subject were chosen due to their location in the brain region containing the lateral geniculate nucleus. These slides were placed under the microscope to determine where the anterior and

posterior poles of the ipsilateral LGN were located in each case. Neurons and blood vessels were traced and numbered under the microscope in a previous study. Surviving cells in the degenerated LGN were measured in millimeters from the center of the surviving cell to the nearest wall of the closest blood vessel. Surviving cells were also noted for the presence or lack of calbindin.

Information about the six subjects' sex, age at lesioning, and number of surviving cells is organized in Table 1. As shown in this table, RHD-4 contains the highest number of surviving cells across all subjects. It also has the greatest number of surviving calbindin-negative cells of any subject. RMS-3, the other adult-lesion subject, has notably greater vascularization as compared with the other subjects. Of the four infant-lesion, RAN-5 had the greatest number of surviving cells, a distinction made important in the results.

Experimental Methods - Distance From Blood Vessel Hypothesis

Chance distances to randomly generated points in the degenerated LGN were compared to quantify whether a neuron's cell body was located closer to a blood vessel than would be expected by chance. Chance was operationally defined as the distance to a blood vessel from a randomized point in the degenerated LGN meant to signify a chance spared cell. To standardize chance distance from a blood vessel, a boxed grid composed of 720 1.8x2.0 cm boxes was created and used to measure the distance from a chance location in the tissue to the nearest traced blood vessel. This grid was numbered from 1 to 720 and encompassed the entire area of the LGN section being measured. Random numbers were generated and used to randomly assign locations from the grid for measurement in the degenerated LGN.

To address the second part of this hypothesis, distances between surviving calbindin-positive neurons and blood vessels in sections of degenerated LGN were compared to the

corresponding distances for calbindin-positive cells at randomly selected points in the DEZ of the intact LGN. In order to measure if the distance between surviving cells in the degenerated LGN was closer to blood vessels than in the corresponding intact LGN, a comparison was performed to see which intact sections corresponded to a degenerated section for each subject. After these relationships were established, the same labelled box grid was used. Random numbers were similarly generated, except in this protocol, a chosen box on the grid was only used if it contained a calbindin-positive cell in the corresponding part of the intact LGN. This was done to account for the inequal distribution of surviving calbindin-positive cells across the degenerated-equivalent zone in the intact LGN.

Experimental Methods - Retinal Innervation Hypothesis

Previously obtained tracings of retinal innervation in the LGN visualized by cholera toxin were used. All monkeys were injected with the cholera toxin six to nine days prior to sacrifice, allowing retinal input to be traced from the retina to the LGN. In five of the six subjects, the injection occurred in the right eye and the visual input from this eye to the left (contralateral) LGN was recorded, resulting in the innervation of layers 1, 4, and 6 in the left LGN of these subjects. This allowed us to see the emergence of new retinal label in the interlaminar zone between layers 2 and 3. In RMS-3, the left eye was injected with cholera toxin as a control and the resulting tracings of the left LGN showed innervation to layers 2, 3, and 5.

Charts were created to find the nearest retinal innervation tracing to each degenerated LGN section. These two images were then overlapped and the calbindin-positive cells were counted based on their location in one of three innervation zones: the S-layer, the zone of high innervation (from Layer 1 to the area between Layers 2 and 3), and all that fell within Layer 3 to

Layer 6. Once every cell was counted, the number that fell within the zone of high innervation was divided by the total number of cells present in the section.

The animal RMS-3 was not used for data analysis in the retinal innervation hypothesis, as it was injected with cholera toxin in the left eye. All five other subjects were injected with cholera toxin in the right eye and the visual input from this eye to the left (contralateral) LGN was recorded, resulting in the innervation of layers 1, 4, and 6 in the left LGN of these subjects. Since the left eye was injected with cholera toxin in RMS-3, this monkey's retinal innervation tracings show innervation to layers 2, 3, and 5, not allowing for visualization of retinal label expansion to the area in between layers 2 and 3 in this subject.

Results

Distance From Blood Vessel Hypothesis

The distances from spared cells to blood vessels in degenerated LGN and distances from randomized points in degenerated LGN to blood vessels were measured for all six subjects. From these measurements, an average distance was calculated for spared cells and randomized points in both infant and adult-lesion as depicted in Figures 3 and 4, respectively. Using a two-tailed t-test corrected for multiple comparisons, the difference between spared cell distance to blood vessel and randomized point to blood vessel for each subject was not significant. However, as shown in Figure 5, the difference in this distance between adult-lesion and infant-lesion subjects was significantly different. As indicated in this figure, adult-lesion subjects were significantly closer to blood vessels than infant-lesion subjects.

The second part of the distance from blood vessel hypothesis is represented with Figure 6: do surviving calbindin-positive cells in the degenerated LGN take better advantage of blood vessels than calbindin-positive cells in the corresponding intact LGN? RMO-6 and RQQ-6 display greater distances from blood vessels in the degenerated LGN than the intact LGN by a significant margin. RAN-5 shows a significantly smaller distance from blood vessels in the degenerated LGN than the intact LGN. No significant difference was observed for RCN-5.

Figures 7 and 8 detail the calbindin contents of the surviving cells in adult- and infant-lesion subjects. In the adult-lesion cases, 81% of all surviving cells were calbindin-positive and 19% were calbindin-negative. In the infant-lesion cases, 98% of all surviving cells were calbindin-positive and 2% were calbindin-negative. A Chi-squared test indicates that this difference in calbindin-negative cell distribution is significant.

Retinal Innervation Hypothesis

According to Figure 9, only RAN-5 displayed a statistically significant change in distribution following V1 lesion. The average percentage of surviving cells in the defined area of high retinal innervation was greater in the degenerated LGN than the intact LGN for infant-lesion subjects RAN-5 and RCN-5 (although not significantly so in RCN-5). RMO-6, RQQ-6, and RHD-4 all displayed a greater average percentage of surviving cells in this zone in the corresponding intact LGN sections compared with the degenerated LGN, although none of these differences were significant. RMS-3 was excluded from these measurements. The percentage of surviving cells in the zone of high retinal innervation in the degenerated LGN tended to be highest at the posterior sections.

Figure 10 maps the distribution of cell location in both the degeneration equivalency zone (DEZ) of intact LGN and the corresponding surviving calbindin-positive cells in degenerated LGN for all infant-lesion subjects. As this figure shows, the difference in distribution following V1-lesion was significantly different in RAN-5, RQQ-6, and RMO-6. However, only RAN-5 experiences an increase in proportion of cells that fall within the zone of high innervation post-lesion to account for this statistically different distribution; in RQQ-6 and RMO-6, the proportion of cells within the high innervation zone decreases. No significant difference was observed for RCN-5.

Discussion

Distance from Blood Vessel Hypothesis

We predicted that surviving calbindin-positive cells in the degenerated LGN would be closer to blood vessels than randomly determined points in the tissue; however, as the results show, there was no significant difference in any subject between the distance from a surviving cell to the nearest blood vessel and the randomized distance to a blood vessel in the degenerated LGN (Figures 3 and 4). In fact, in all subjects except RAN-5 and RHD-4, surviving cells were farther on average from blood vessels than chance. While surviving cells in RAN-5 and RHD-4 were closer to blood vessels than chance, none of these differences were great enough to be statistically significant.

Since blood vessels provide essential oxygen and nutrients to cells in the LGN, we hypothesized that the ones that survive V1-lesion would do so based on their preferential location to these resources. Based on Figures 3 and 4, this does not seem to be the case for these six subjects – in both adult and infant-lesion cases, there is no significant evidence that surviving cells are preferentially located to blood vessels with regards to chance. However, when comparing across age in Figure 5, the average distance from a surviving cell to the nearest blood vessel in adult-lesion animals was 0.16 mm, while the same average distance in our infant-lesion animals was 0.23 mm. A two-tailed T test indicates that the difference between these two means is statistically significant.

This could mean that adult-lesion monkeys take better advantage of blood vessels than infant-lesion animals. However, it is also possible that surviving cells in adult-lesion animals are closer to blood vessels because there is a greater density of blood vessels to choose from in these adults. While the literature reports that cerebral blood flow is significantly reduced in aged

humans compared to young adults (Sonntag et al., 2007), aged macaque monkeys seem to have a significant vascularization response to traumatic brain injury. In a previous study involving these same six monkeys, the number of blood vessels per square millimeter in the degenerated LGN was compared to the number of blood vessels per square millimeter in the intact LGN. Adult-lesion cases RHD-4 and RMS-3 skyrocketed from 3 per square millimeter in the intact side to 6 and 10 per square millimeter post-lesion, respectively, while the infant cases ranged 3-5 blood vessels per square millimeter and exhibited no significant differences between intact and degenerated (Knudson & Rodman, unpublished data). This suggests an underlying difference in vascularization following traumatic brain injury between the two age groups, which would account for the increase in blood vessels and the decrease in distance from surviving cell to blood vessel.

This result from Figure 5 may also be a result of the strong sensitivity to degeneration damage infants experience compared to adults. However, cortical plasticity is also incredibly strong at infancy and is less present through the aging process, which would account for its significantly greater presence of calbindin-positive surviving cells in our infant cases than the adults. Although the infant brain is more greatly affected by traumatic injury, it is more capable of recovery than adults; old age is consistently associated with poor recovery from brain injury (Atapour et al., 2017). The plasticity of the LGN allows infant animals who suffer a traumatic brain injury to utilize new thalamic connections and alternative pathways to recover from injury (Mikellidou, 2017).

Figure 6 displays the results of our comparison of surviving calbindin-positive cells distance from blood vessels in the degenerated LGN and the intact LGN. We only obtained data for the four infant-lesion cases; in three of these four cases, the distance to blood vessels in the

degenerated LGN was greater than the distance in the intact LGN (significantly so for RMO-6 and RQQ-6). RAN-5 was the only exception and displayed a significantly greater distance to blood vessels in the intact LGN than the degenerated LGN, which is the trend we initially predicted. Interestingly, this data suggests that surviving, calbindin-positive cells in the degenerated LGN of infants are actually farther from blood vessels than their control counterparts in the intact LGN.

As such, both of our experiments for the blood vessel distance hypothesis returned results contrary to our initial expectations. Taking these results together, the data suggests that surviving cells in the degenerated LGN following V1 lesion: were not significantly closer to blood vessels than chance and were not significantly closer to blood vessels than their corresponding intact LGN sections. There are several reasons this could be the case. If blood vessels provide no protective benefit to survival after degeneration, there would be no reason for cells to preferentially cluster around them. There are other neuroprotective factors that may be more of an influence on the survival of these LGN cells post-lesion; the protective steroid hormones progesterone and estrogen have both been indicated in survival following lesion to primary visual cortex (Pardue and Rachael, 2018). Additionally, the surviving cells could be surviving due to their location within a zone of retinal input and thus relatively unaffected by lack of proximity to blood vessel.

Figures 7 and 8 display the number of calbindin-positive vs calbindin-negative cells in both the adult and infant-lesion cases. While only 2% of the surviving cells in infant-lesion cases were calbindin-negative, 19% of the surviving cells in adult-lesion cases were calbindin-negative, a difference that is statistically significant. The presence of calbindin is an indisputable benefit to degeneration survival; calbindin is not only a marker for the koniocellular pathway, it

is a protein thought to play a neuroprotective role in cell survival (Sorenson, 1999). One of the factors that determines neural susceptibility to disease is toxic buildup in intracellular calcium, which calcium-binding proteins like calbindin help to buffer (Fairless et al., 2019). The significantly greater proportion of calbindin-negative cells that survive degeneration in adult-lesion animals indicates the possibility of a different type of cell in these animals that survives V1 lesion.

Retinal Innervation Hypothesis

We predicted that cells located in a specified area of high retinal innervation would be more likely to survive due to the continued stimulation and supply of visual input. Since we know that new zones of high innervation appear in the interlaminar zone between Layers 2 and 3 following lesion to V1, we hypothesized there would be a proportionally large number of cells that survive in this area taking advantage of this cortical plasticity in the retinotopic representation of the LGN. Figure 9 displays the results of the retinal innervation hypothesis: two of the five subjects, RAN-5 and RCN-5 display the hypothesized trend where a greater percentage of surviving cells fell within this privileged-position retinal innervation zone than did cells in the corresponding intact LGN section. However, only RAN-5 displays this behavior at a statistically significant level. RMO-6, RQQ-6, and RHD-4 did not preferentially show a greater percentage of surviving cells in this innervation zone in degenerated tissue compared with intact.

As shown in Figure 10, the distribution of cell location following V1 lesion was significantly different in RAN-5, RMO-6, and RQQ-6. However, this change in distribution was not necessarily due to a predicted increase in cell proportion in the zone of high innervation. While the proportion of innervation-privileged cells did increase in RAN-5, this proportion decreased in both RMO-6 and RQQ-6. In RMO-6, the biggest change in distribution post-lesion

was the increase in proportion of cells in the S-layer; in RQQ-6, this change in distribution saw a large increase in proportion of cells falling within the defined Other area (from layer 3 to layer 6). This seems to indicate that the change in cell location distribution post-lesion in this experiment was not associated with an increase in cell proportion in any specific defined area of the LGN, as it occurs in a different area for each subject. As such, the data does not indicate any consistent significant preference for cells to be preferentially located in this area of high retinal innervation following lesion as compared with the unlesioned intact LGN.

The proportion of innervation-privileged cells in any given section from any subject ranged from 11% to 67%. Of all four subjects, there were only four individual LGN sections in which the proportion of innervation-privileged cells was greater than the proportion of surviving cells falling elsewhere in the LGN – and three of these four sections belonged to subject RCN-5. RCN-5, though not displaying a statistically significant difference in innervation-privileged cells post-lesion, demonstrated generally strong surviving cell presence in this innervated zone, with an average of 51.4% of surviving cells existing between Layer 1 and the interlaminar zone between Layers 2 and 3. RCN-5 was the smallest infant with only 106 surviving calbindin-positive cells, the fewest of any subject. Additionally, RCN-5 was one of the female subjects and may have experienced the neuroprotective effects of estrogen post-lesion, as described previously.

RAN-5 saw the greatest statistically significant increase in innervation-privileged cells post-lesion, with an increase from 27.5% in the intact LGN to 36% in the degenerated LGN. Comparing this trend with those of RAN-5's fellow subjects, there are possible explanations as to how this subject could have been taking such greater advantage of highly innervated zones. Being an infant-lesion subject, it is possible that RAN-5 had the greatest instance of cortical

plasticity and experienced the most successful rearrangement of high innervation zones post-lesion. As mentioned above, cortical plasticity tends to be strongest in the young. Unlike RCN-5, RAN-5 was a male and contained over 400 surviving calbindin-positive cells. The main commonality between these two is their status as infant-lesion cases, which may generally speak to the greater ability of infant brains to adapt to maladaptive change. The other three cases, two infants and one adult, show a decrease in innervation-privileged cells as compared with their corresponding intact LGN sections. The cells that survive in these subjects appear to be more concentrated in other regions of the LGN; in RMO-6, a large number of the surviving cells were grouped towards the upper (dorsal) part of the LGN, while surviving cells in RQQ-6 appear to be primarily found around the S-layer (the region below Layer 1). While there is retinal innervation to both of these other areas, the interlaminar zone between layers 2 and 3 is the primary location in which, post lesion, new bands of high innervation consistently appear, thus it was our focus. Despite the promising results of RAN-5 and RCN-5, there is no conclusive and consistent indication that the proportion of innervation-privileged neurons was significantly greater than the proportion that fell outside of these zones in our sample of macaque monkeys.

Implications of Blindsight Research

The study of blindsight has implications in the rehabilitation of those with traumatic brain injury: "… blindsight has clinical importance because restoration of visual function, even in the form of blindsight, may improve quality of life in hemianopic [blindness over half the field of vision] patients" (Yoshida, Hafed, and Isa, 2017). In these patients, there can be a significant decrease in quality of life, causing deficiencies in driving, reading, and navigation (Goodwin, 2014). As such, the primary goal is to utilize implicit visual function to restore explicit visual detection and achieve the most visual capability with what visual functions remain. Additionally,

blindsight raises fascinating questions about the dichotomy present between vision and awareness. While the core phenomenology of visual experience has been said to be primarily incited by the external object, blindsight makes a case for a visual experience without awareness of this external object (Brewer, 2007). In blindsighted individuals, it is the feeling of something being present that has no distinct shape or color; these patients would report seeing the motion of objects as "like a shadow" with no defining shape or form (Brogaard, 2015).

Vision and attention are closely related, allowing attentional modulation to occupy an important piece of our conscious visual experience. Even without a condition like blindsight, the human brain routinely filters out information that is not salient and selects the data that will be useful for survival. The information that is filtered out has still, on some subconscious level, been perceived and analyzed as to not be brought into conscious attention. While attention and consciousness have a somewhat contentious relationship, it has been shown that attention modulates response in visual cortex, exstrastriate cortex, and the LGN. In an individual with blindsight, this dichotomy is more pronounced and can yield further clarifications on the exact nature of vision's relationship with awareness and attention.

There are some noteworthy limitations to this project. In the retinal innervation hypothesis, the retinal innervation tracings outlined a section of the brain in a slightly different location than the dLGN section, so they did not perfectly overlap. This may have resulted in underrepresentation of surviving cells in innervation zones when counting. Also, the retinal innervation tracings only indicated zones of input for the right (contralateral) eye; therefore, it is possible that the surviving cells that did not align with zones in the innervation tracing were in a zone of retinal input for the left (ipsilateral) eye. Additionally, we discovered the uneven spread of the surviving LGN cells in degenerated tissue following the first round of data collection for

degenerated LGN versus chance. As such, we could not account for the skewed distribution of surviving cells in these measurements, although we later corrected our measuring techniques when comparing degenerated LGN to corresponding intact LGN to account for this discrepancy.

Given the general variability in results, it is important to note the individual variability in subjects. As discussed above, age, sex and vascularization are variables that could have an impact on the survival capability for an individual. Additionally, due to the partial nature of the unilateral lesions administered to each subject, there is variability in lesion size and location that can account for differences in LGN degeneration and surviving cell location. As such, these subjects and their various pre- and post-morbid differences display the wide variability possible in blindsight and the individuality of each case.

Conclusion

The overall results of this experiment do not implicate blood vessels in the survival of calbindin-positive cells post V1-lesion, as surviving cells were not significantly closer to blood vessel than would be expected by chance or than the calbindin-positive cells in a corresponding intact LGN section. Retinal innervation does not appear to occur at a higher proportion in the designated zone of high retinal innervation than in the rest of the LGN, and innervation-privileged cells were not found at a higher proportion post-lesion than in the corresponding intact LGN. However, the distance from spared cell to nearest blood vessel was significantly smaller in adult-lesion animals as compared with infant-lesion animals, and these adult-lesion animals displayed a significantly greater proportion of surviving calbindin-negative cells.

As such, I would be interested in taking a closer look at this individual variability in a future experiment and isolating the variable of age in order to see if there truly are differences in mediated visual capacity. This would involve taking a closer look at these calbindin-negative

surviving cells: do they tend to cluster in specific regions of the LGN, are they morphologically distinct, and could they be indicative of non-K cells surviving degeneration? Besides age, individual variables such as sex, vascularization, and premorbid differences in strength of retinal input warrant further investigation. Another possible next experiment would be to see if dendritic branching of surviving cells post-lesion is significantly longer or more intimately wrapped around a blood vessel than cells in the intact LGN, allowing certain cells a greater chance at survival. This would account for the lack of a proximity-based relationship between cells and blood vessels found in this experiment; if longer dendrites are prominent following lesion, surviving neurons could be a great distance from a blood vessel and still take full advantage of the blood vessel's nutrients, oxygen, and glucose.

Tables and Figures:

Name of Subject	Sex	Age at lesioning	# of surviving calbindin-positive cells	# of surviving calbindin-negative cells	# of total surviving cells
RMO-6	Male	36 days	267	10	277
RAN-5	Male	47 days	465	5	470
RQQ-6	Female	38 days	153	5	158
RCN-5	Female	45 days	107	3	110
RHD-4	Female	4.9 years	442	122	564
RMS-3	Male	5.9 years	406	79	485

Table 1. This table displays identifying information about each subject used in this experiment. Subjects shaded in blue were lesioned in adulthood, while subjects shaded in yellow were lesioned at infancy.

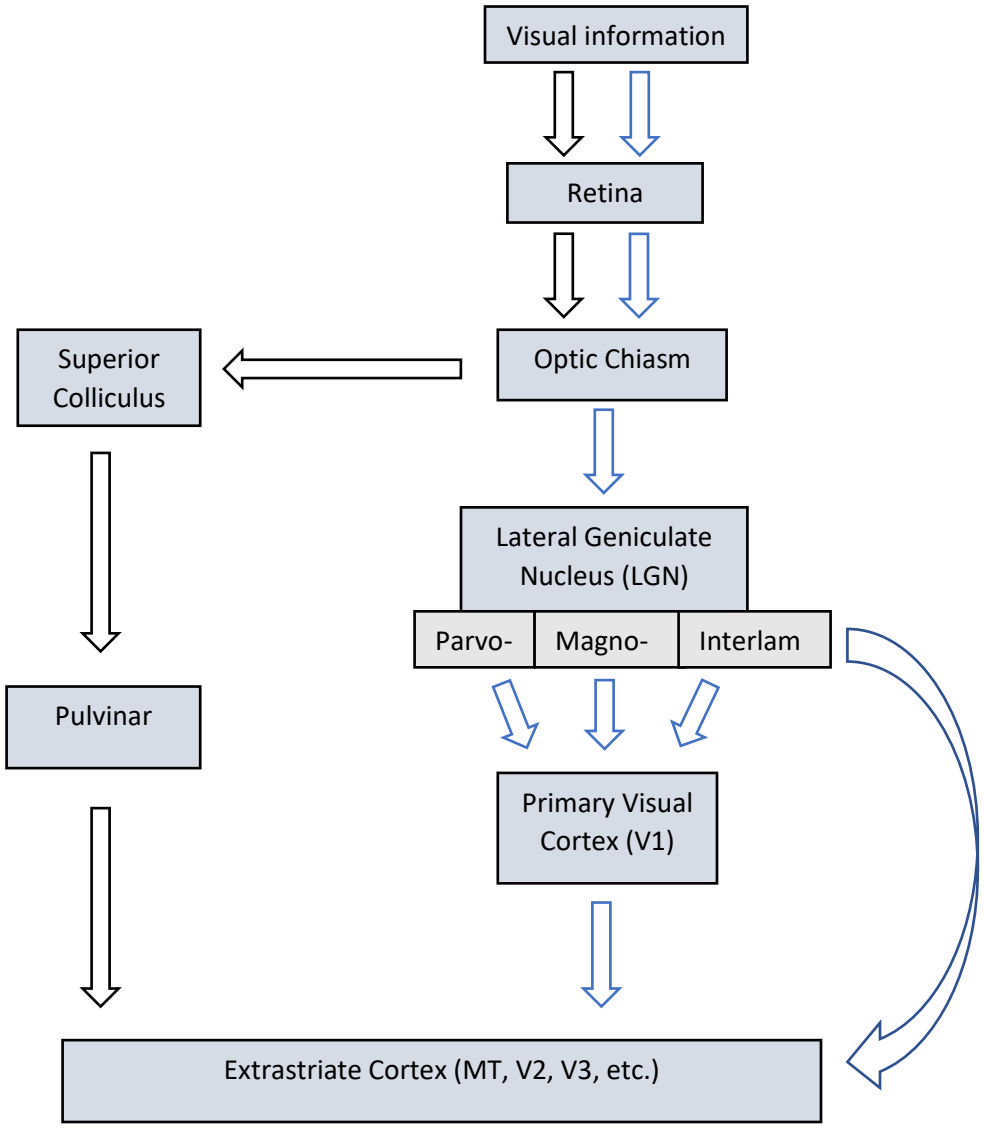

Figure 1. This figure displays the primary and secondary visual pathways. The primary visual pathway is indicated with blue arrows and the secondary visual pathway is indicated with black arrows.

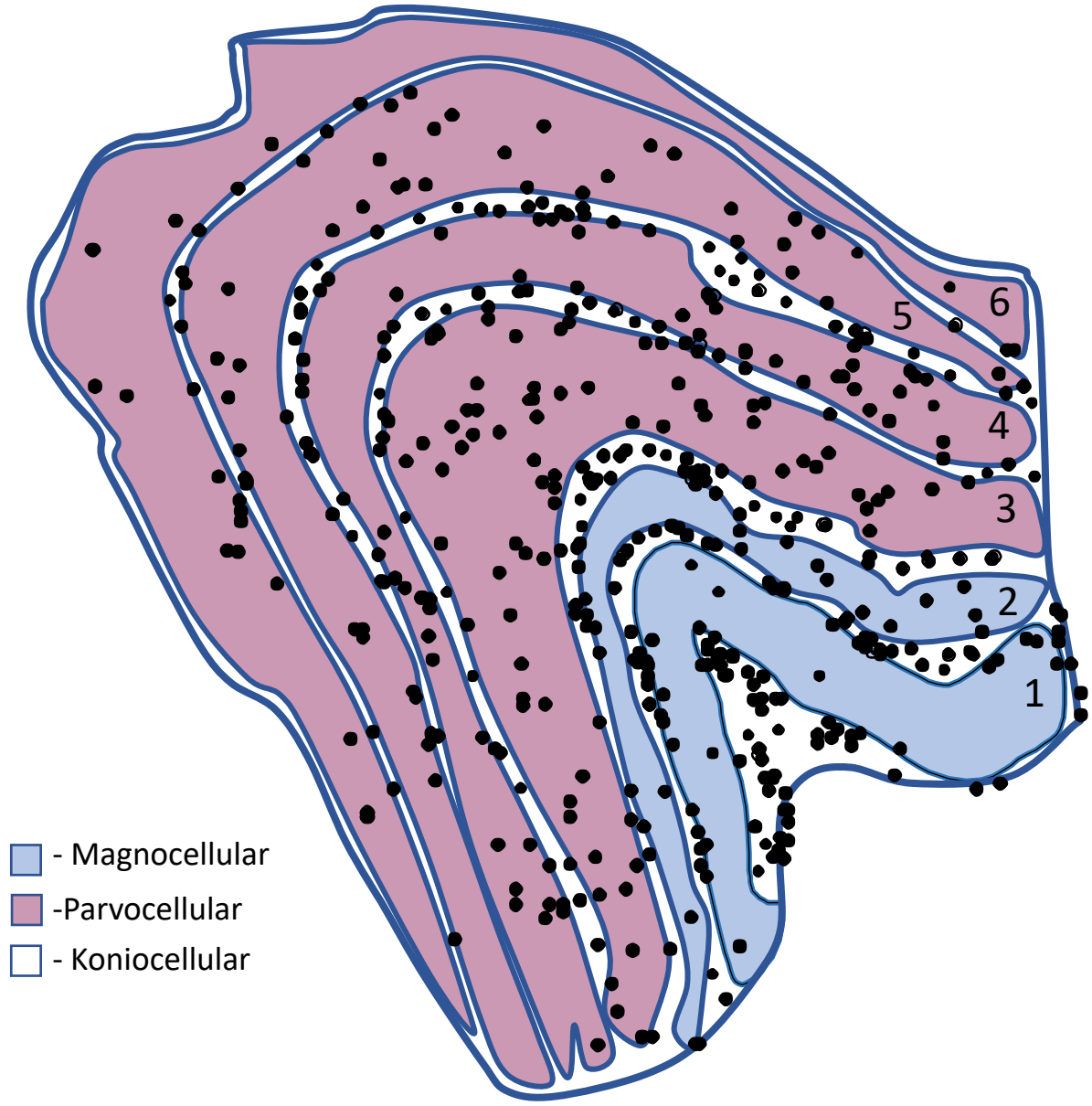

Figure 2. This figure is a tracing from an intact LGN section of subject RMS-3. The layers have been numbered 1-6, with the magnocellular layers indicated in orange and the parvocellular layers indicated in blue. Interlaminar layers lie within the white areas between colored layers.

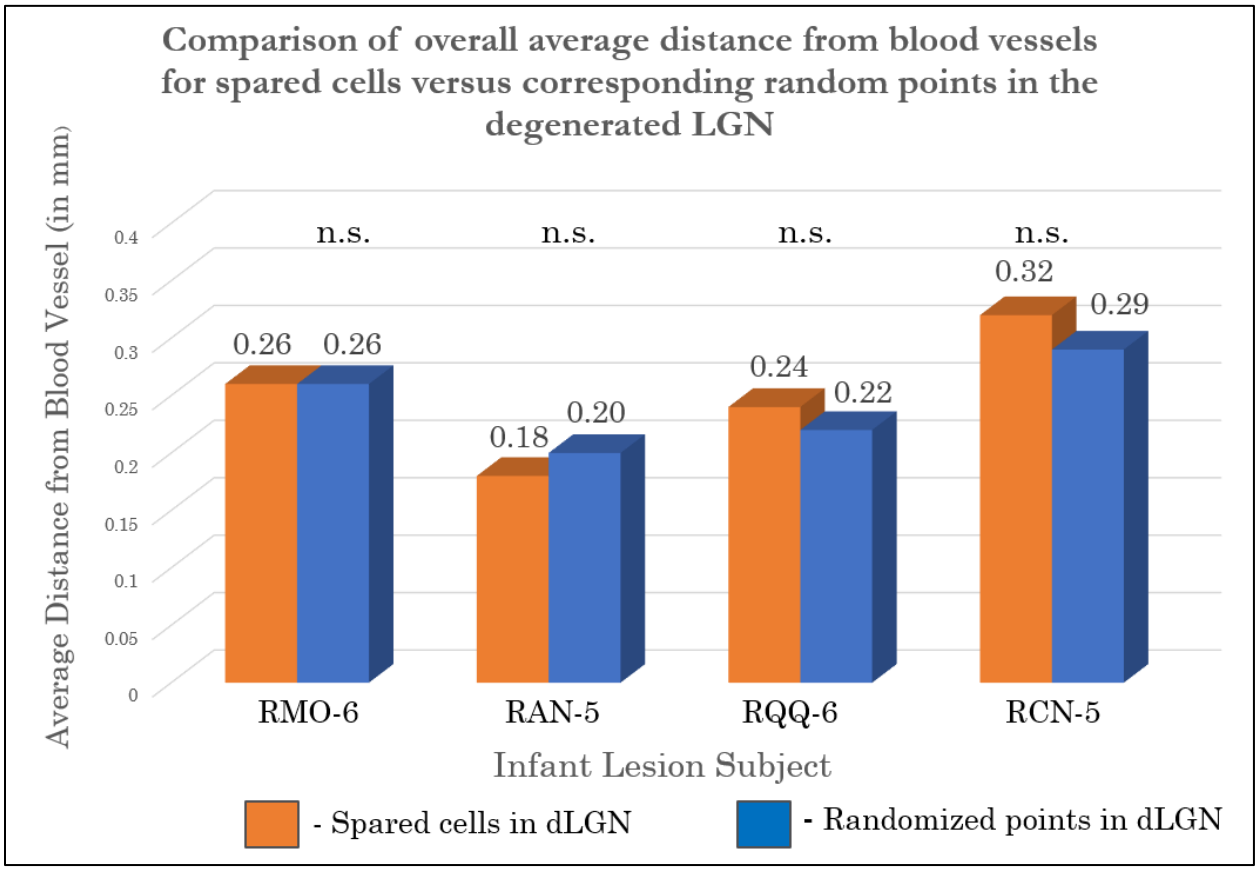

Figure 3. A comparison of overall average distance from blood vessels in both spared cells and corresponding random points in all infant-lesion cases. A two-tailed t-test was performed for each subject and indicated no significant difference between the values for spared cells and for randomized points in the degenerated tissue in any subject.

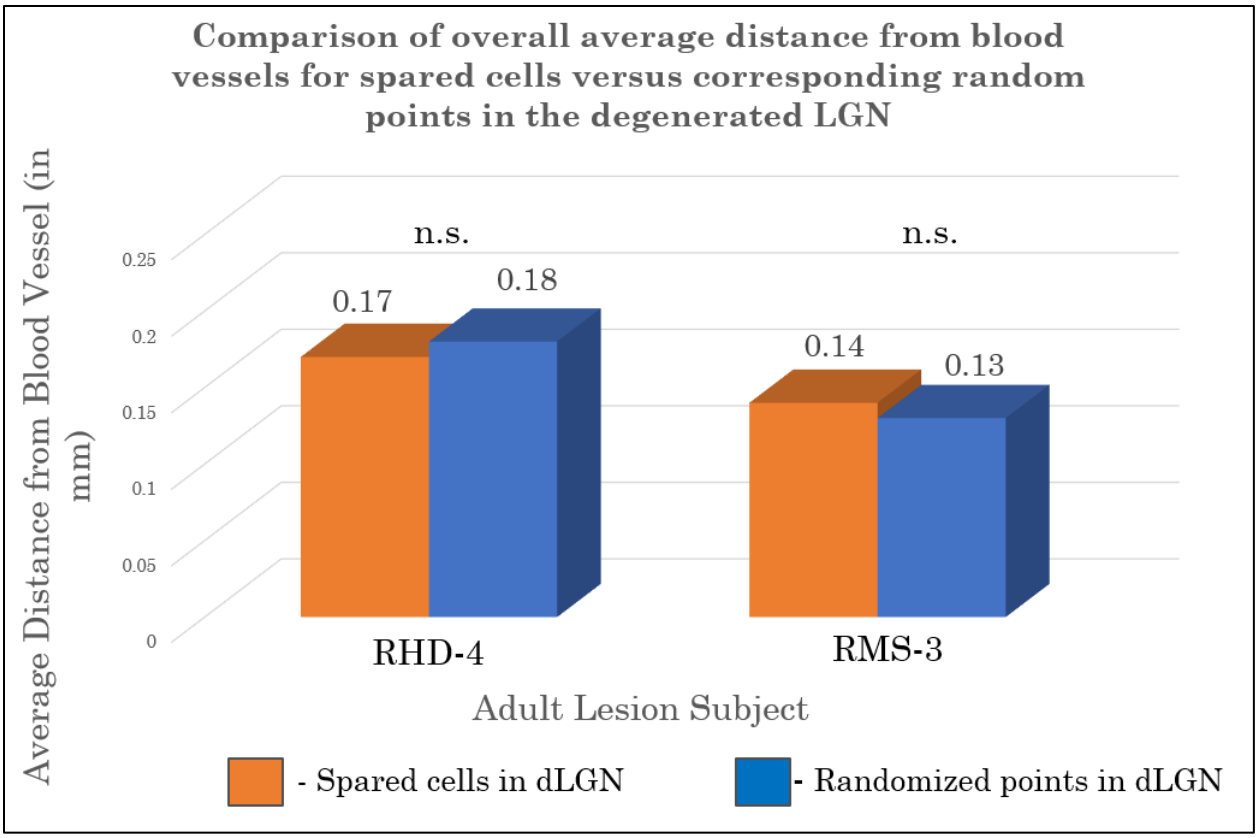

Figure 4. A comparison of overall average distance from blood vessels in both spared cells and corresponding random points in all adult-lesion cases. A two-tailed t-test was performed for each subject and indicated no significant difference between the values for spared cells and for randomized points in the degenerated tissue in any subject.

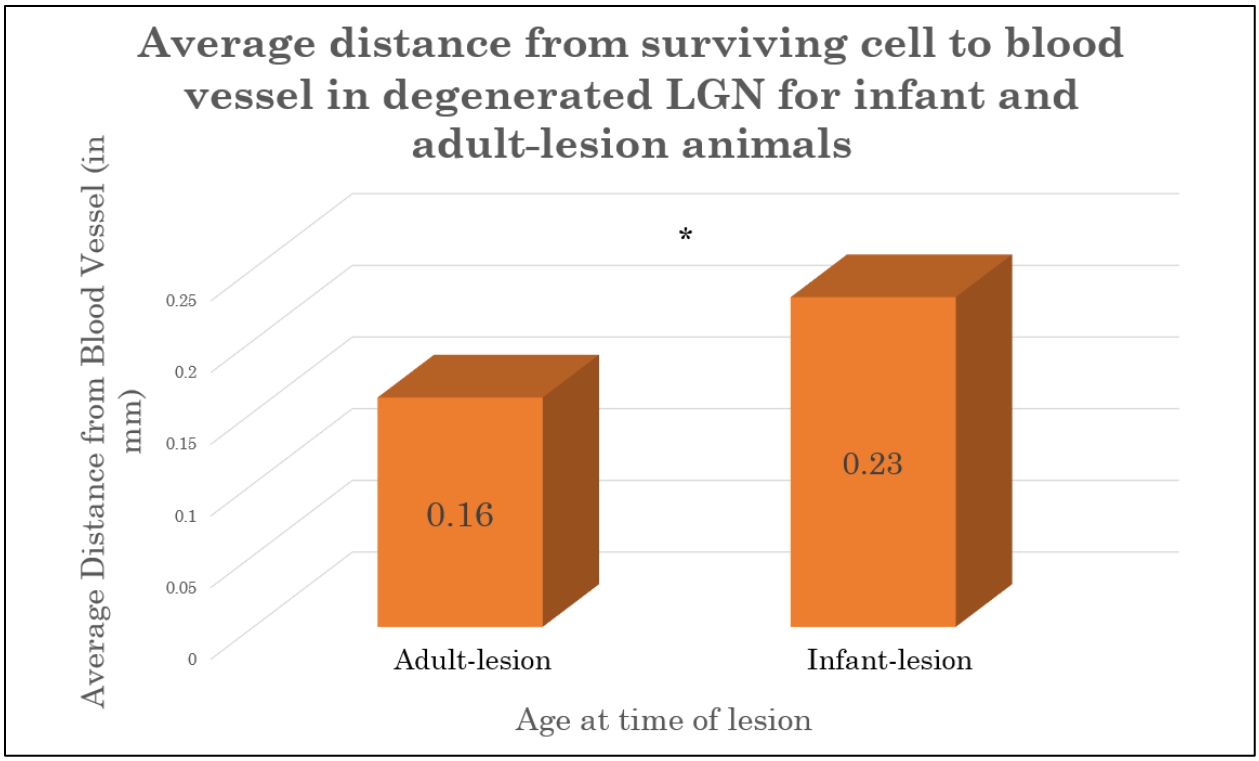

Figure 5. The average distance from surviving cell to blood vessel in degenerated LGN in both adult- and infant-lesion cases. A two-tailed t test was performed and the difference between these two values was found to be statistically significant ($t = 10.12$, $p < 0.0001$) .

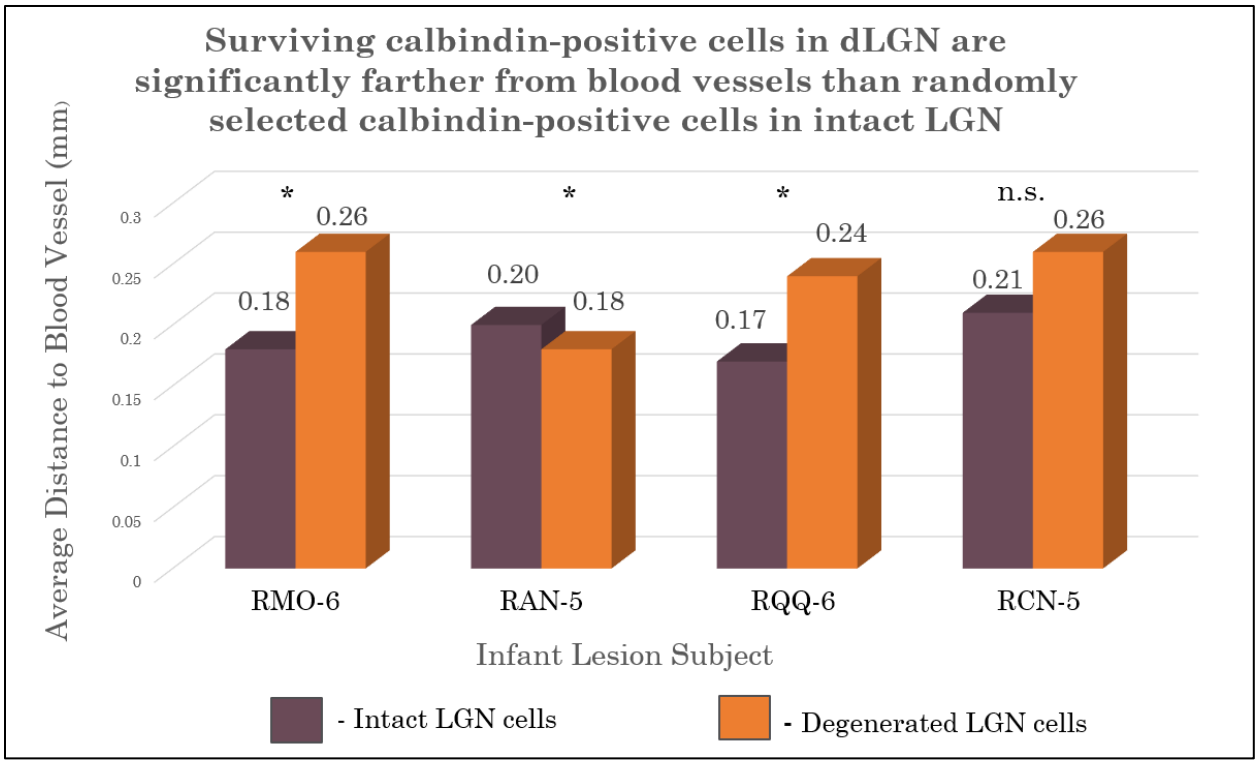

Figure 6. A comparison of surviving calbindin-positive cells in the degenerated LGN tissue to randomly selected calbindin-positive cells in the intact LGN for infant-lesion subjects. A two-tailed t-test was performed for each subject and indicated a significant difference for RMO-6 ($t = -6.57$, $p < 0.00001$), RAN-5 ($t = 2.28$, $p = 0.023$), and RQQ-6 ($t = -3.28$, $p = 0.0011$). No significant difference was observed for RCN-5.

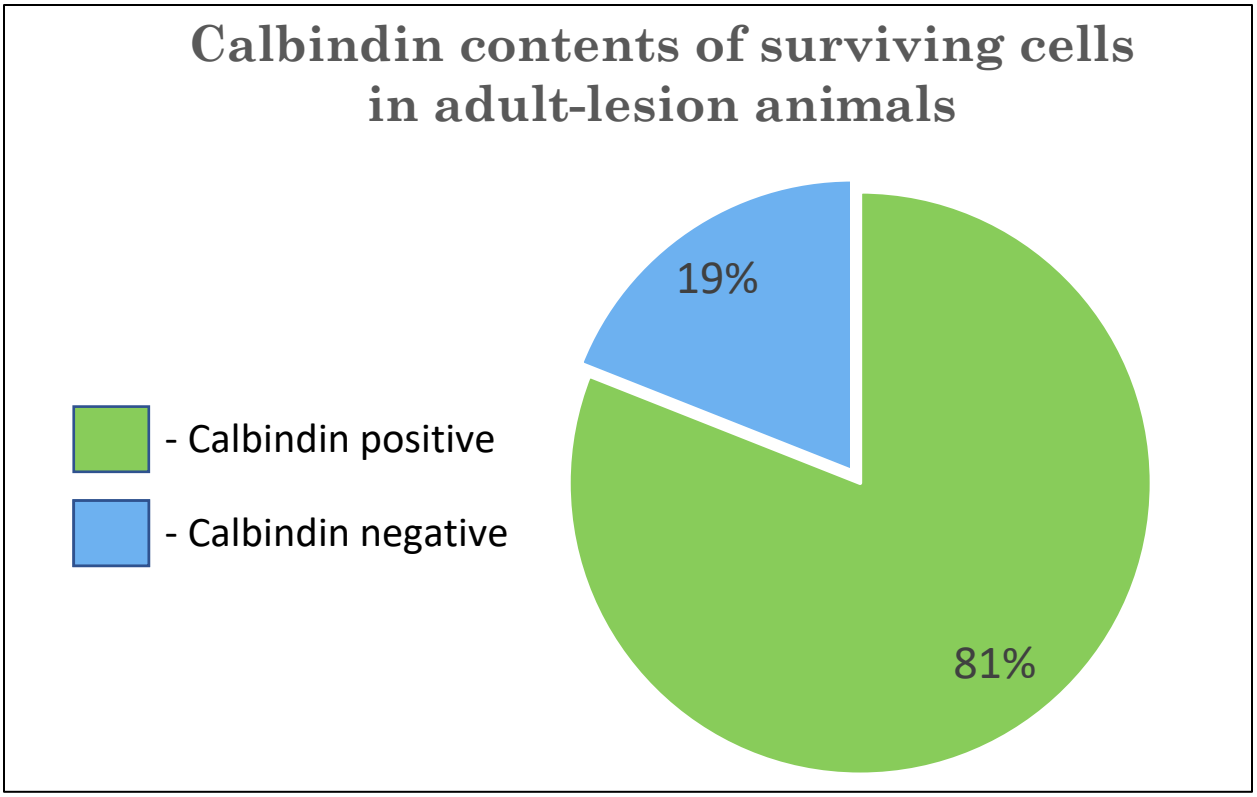

Figure 7. This figure represents the calbindin contents of surviving cells in the degenerated LGN in adult-lesion cases RHD-4 and RMS-3. The green shaded area represents calbindin-positive surviving cells and the blue shaded area represents calbindin-negative surviving cells.

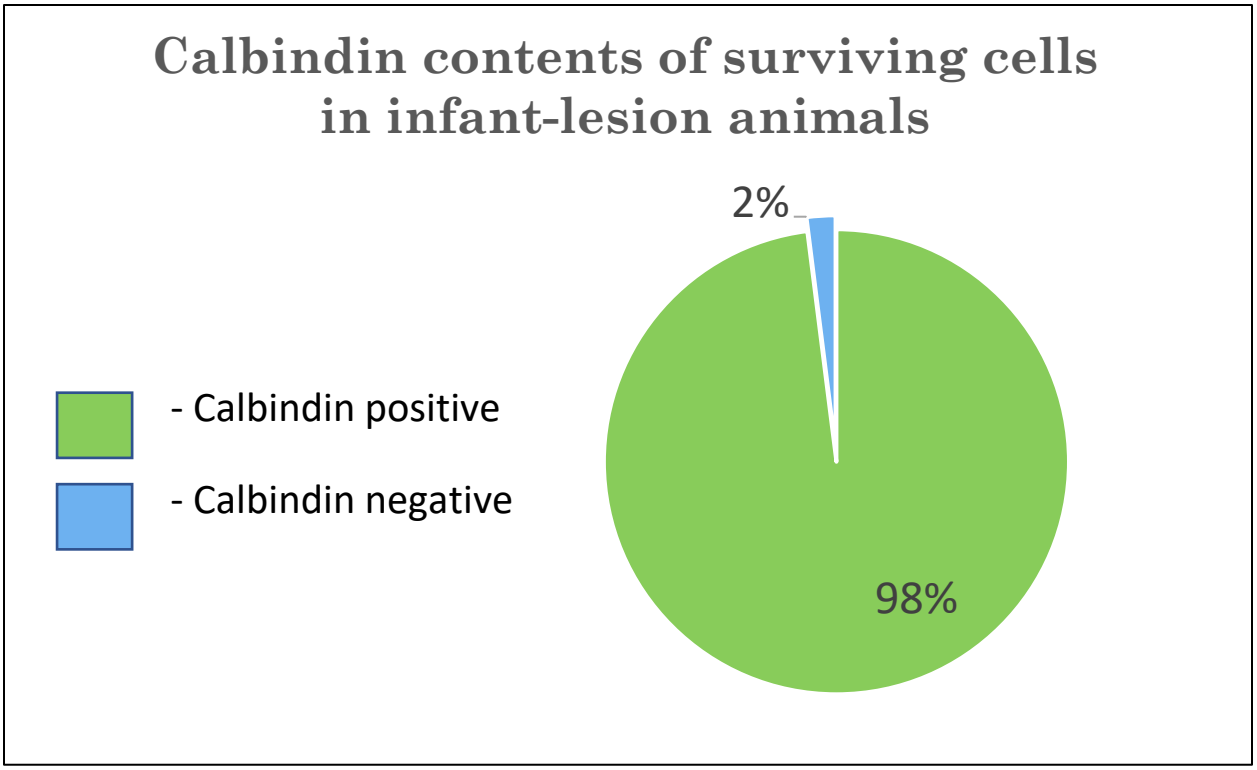

Figure 8. This figure represents the calbindin contents of surviving cells in the degenerated LGN in all infant-lesion cases. The difference between adults (Figure 7) and infants (Figure 8) in proportion of calbindin-negative surviving cells to total surviving cells is significantly different, X^2 (1, N = 2,064) = 123.86, p < .00001.

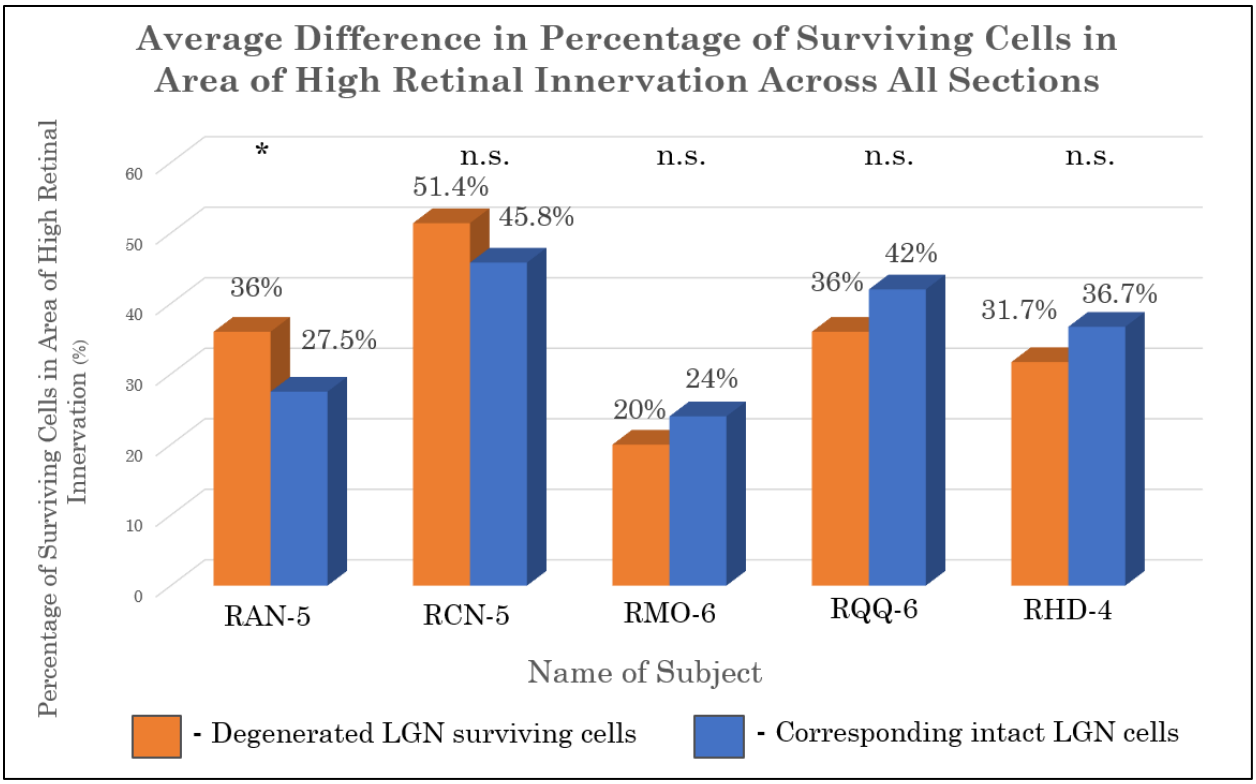

Figure 9. This figure represents the percentage of surviving cells in the degenerated LGN that fall within a defined zone of high retinal innervation as compared with the percentage of cells in the corresponding intact LGN that fall within this zone. A Chi-squared test was conducted to measure the differences in distribution for each subject – only the difference in distributions for RAN-5 were significantly different, X^2 (1, N = 888) = 12.34, p = .00044.

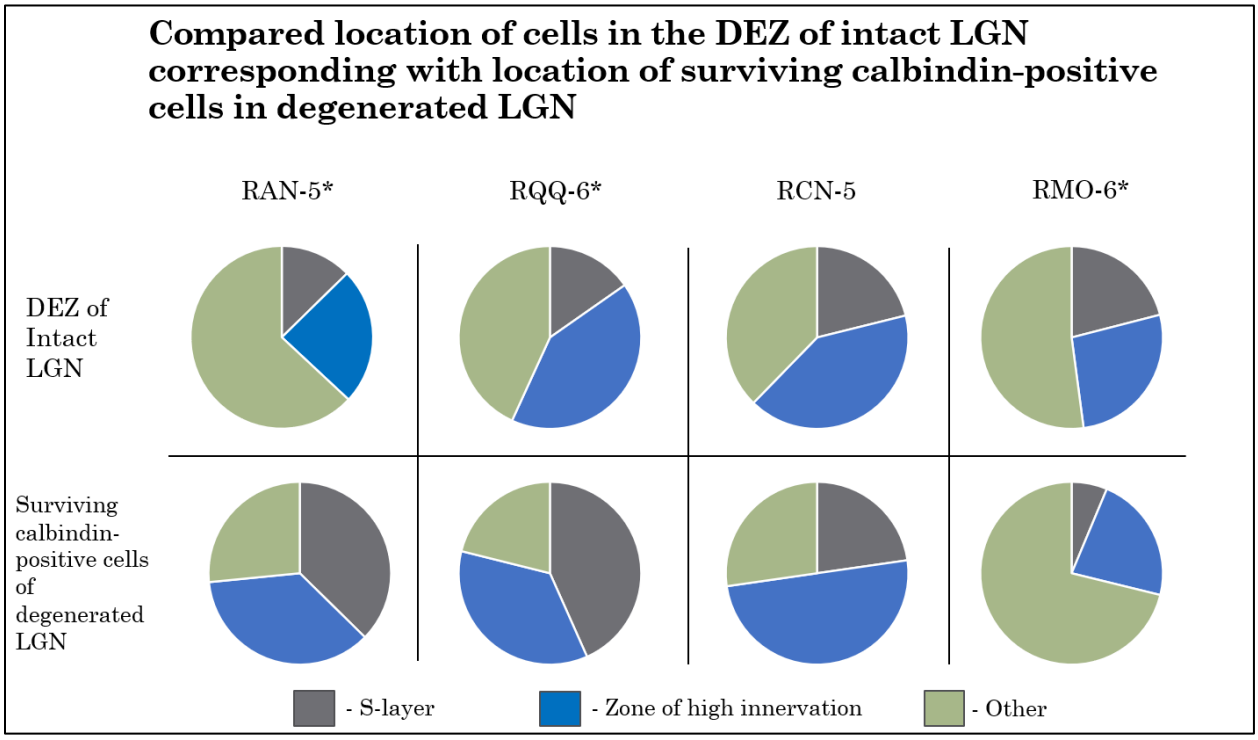

Figure 10. This figure represents the distribution of cell location in both: the degeneration equivalency zone of the intact LGN and the corresponding surviving calbindin-positive cells in degenerated LGN. The gray portion indicates cells that fall within the S-layer, the blue indicates cells falling within the predefined zone of high innervation (from Layer 1 to the area in between layers 2 and 3), and the green indicates cells falling outside these regions. A Chi-squared test was performed and a significant difference between distributions was observed with RAN-5, X^2 (2, N = 888) = 101.15, p < 0.00001, RQQ-6, X^2 (2, N = 574) = 40.29, p < 0.00001, and RMO-6, X^2 (2, N = 865) = 32.43, p < 0.00001.. No significant difference in distributions was observed for RCN-5.

References

Ajina, S., Bridge, H. (2016). Blindsight and Unconscious Vision: What They Teach Us about the Human Visual System. The Neuroscientist : a review journal bringing neurobiology, neurology and psychiatry, 23(5), 529–541.

Ajina, S., Bridge, H. (2018). Blindsight relies on a functional connection between hMT+ and the lateral geniculate nucleus, not the pulvinar. PLoS biology, 16(7), e2005769.

Andreone, B. J., Lacoste, B., and Gu, C. (2015). Neuronal and vascular interactions. Annual review of neuroscience, 38, 25–46.

Atapour, N., Worthy, K. H., Lui, L. L., Yu, H., and Rosa, M. G. (2017). Neuronal degeneration in the dorsal lateral geniculate nucleus following lesions of primary visual cortex: Comparison of young adult and geriatric marmoset monkeys. Brain Structure and Function, 222(7): 3283-3293.

Azzopardi, P., and Cowey, A. (1998). Blindsight and visual awareness. Consciousness and Cognition, 7(3): 292-311.

Brewer, B. (2007). Perception and its objects. Philosophical Studies, 132(1), 87–97.

Brogaard, B. (2015). Type 2 blindsight and the nature of visual experience. Consciousness and Cognition, 32: 92-103.

Carsten, K., Evrard, H. C., Shapcott, K. A., Haverkamp, S., Logothetis, N. K., & Schmid, M. C (2016). Cell-Targeted Optogenetics and Electrical Microstimulation Reveal the Primate Koniocellular Projection to Supra-granular Visual Cortex. Neuron, 90(1): 143–151. Published online 2016 Mar 24.

Chariker, L., Shapley, R., & Young, L. S. (2016). Orientation Selectivity from Very Sparse LGN Inputs in a Comprehensive Model of Macaque V1 Cortex. The Journal of Neuroscience, 36(49), 12368–12384.

Dineen, J., Keating, E. G. (1981). The primate visual system after bilateral removal of striate cortex. Survival of complex pattern vision. Exp Brain Res. 41(3-4):338-45.

Eiber, C. D., Rahman, A. S., Pietersen, A. N., Zeater, N., Dreher, B., Solomon, S. G., & Martin, P. R. (2018). Receptive field properties of koniocellular on/off neurons in the lateral geniculate nucleus of marmoset monkeys. The Journal of Neuroscience, 38(48): 10384–10398.

Eichmann, A., & Thomas, J. L. (2013). Molecular parallels between neural and vascular development. Cold Spring Harbor perspectives in medicine, 3(1).

Fairless, R., Williams, S. K., & Diem, R. (2019). Calcium-Binding Proteins as Determinants of Central Nervous System Neuronal Vulnerability to Disease. International journal of molecular sciences, 20(9), 2146.

Freud, E., Culham, J. C., Plaut, D. C., & Behrmann, M. (2017). The large-scale organization of shape processing in the ventral and dorsal pathways. eLife, 6, e27576.

Goodwin D. (2014). Homonymous hemianopia: challenges and solutions. Clinical ophthalmology (Auckland, N.Z.), 8, 1919–1927.

Gross, C. G., Moore, T., & Rodman, H. R. (2004). Visually guided behavior after V1 lesions in young and adult monkeys and its relation to blindsight in humans. Progress in Brain Research, 19(144): 279-294.

Hendrickson, A., Warner, C. E., Possin, D., Huang, J., Kwan, W. C., & Bourne, J. A (2015). Retrograde transneuronal degeneration in the retina and lateral geniculate nucleus of the V1-lesioned marmoset monkey. Brain Structure and Function, 220(1): 351–360.

Mikellidou, R. Arrighi, G. Aghakhanyan, F. Tinelli, F. Frijia, S. Crespi, F. De Masi, D. Montanaro, M. C. Morrone. Neuropsychologia. 2017 Oct 31

Pardue, M. T., & Allen, R. S. (2018). Neuroprotective strategies for retinal disease. Progress in retinal and eye research, 65, 50–76.

Pfisterer, U., & Khodosevich, K. (2017). Neuronal survival in the brain: neuron type-specific mechanisms. Cell Death and Disease, 8: 1-13.

Riddoch, G. (1917). Dissociation of visual perceptions due to occipital injuries, with especial reference to appreciation of movement. Brain: A Journal of Neurology, 40: 15-57.

Rodman, H. R., Sorenson, K. M., Shim, A. J., & Hexter, D. P. (2001). Calbindin immunoreactivity in the geniculo-extrastriate system of the macaque: implications for heterogeneity in the koniocellular pathway and recovery from cortical damage. The Journal of Comparative Neurology, 431: 168-181.

Rodman, H.R. (2006) Behavioral and neural alterations following V1 damage in immature primates. In: S. G. Lomber and J.J. Eggermont (eds.), Reprogramming the cerebral Scortex: plasticity following central and peripheral lesions. Oxford: Oxford University Press: 89-111.

Schmid, M. C., Mrowka, S. W., Turchi, J., Saunders, R. C., Wilke, M., Peters, A. J., . . . Leopold, D. A. (2010). Blindsight depends on the lateral geniculate nucleus. Nature, 466(7304): 373-377.

Solomon, S. G., & Rosa, M. G. (2014). A simpler primate brain: the visual system of the marmoset monkey. Frontiers in neural circuits, 8, 96.

Sonntag, W. E., Eckman, D.M., Ingraham. J., et al. Regulation of Cerebrovascular Aging (2007). In: Riddle DR, editor. Brain Aging: Models, Methods, and Mechanisms. Boca Raton (FL): CRC Press/Taylor & Francis.

Sorenson, K. (1999). The role of the visual thalamus in residual vision after primary visual cortex lesion in infant and adult macaques. Emory Theses and Dissertations, 1-135.

Stoerig, P., & Cowey, A. (1997). Blindsight in man and monkey. Brain, 120: 535-559.

Yoshida, M., Hafed, Z. M., & Isa, Tadashi. Informative cues facilitate saccadic localization in blindsight monkeys. Frontiers in Systems Neuroscience, 11(5): 1-11.

Yu, H., Atapour, N., Chaplin, T. A., Worthy, K. H., & Rosa, M. G. (2018). Robust Visual Responses and Normal Retinotopy in Primate Lateral Geniculate Nucleus following Long-term Lesions of Striate Cortex. The Journal of Neuroscience, 38(16): 3955-3970.